

CD36 deletion ameliorates diabetic kidney disease by restoring fatty acid oxidation and improving mitochondrial function

Huimin Niu^{a,b}, Xiayu Ren^a, Enxue Tan^a, Xing Wan^a, Yu Wang^a, Honghong Shi^a, Yanjuan Hou^a and Lihua Wang^a

^aDepartment of Nephrology, Second Hospital, Shanxi Medical University, Taiyuan, China; ^bDepartment of Nephrology, Heping Hospital Affiliated to Changzhi Medical College, Changzhi, China

ABSTRACT

Renal tubular epithelial cells (TECs) are vulnerable to mitochondrial dysregulation, which is an integral part of diabetic kidney disease (DKD). We found that CD36 knockout ameliorated mitochondrial dysfunction and diabetic kidney injury in mice, improved renal function, glomerular hypertrophy, tubular injury, tubulointerstitial fibrosis, and kidney cell apoptosis. Furthermore, CD36 knockout conferred protection against diabetes-induced mitochondrial dysfunction and restored renal tubular cells and mitochondrial morphology. CD36 knockout also restored mitochondrial fatty acid oxidation (FAO) and enhanced FAO-associated respiration in diabetic TECs. CD36 was found to alter cellular metabolic pathways in diabetic kidneys partly *via* PDK4 the -AMPK axis inactivation. Because CD36 protects against DKD by improving mitochondrial function and restoring FAO, it can serve as a potential therapeutic target.

ARTICLE HISTORY

Received 26 July 2023
Revised 14 November 2023
Accepted 4 December 2023

KEYWORDS

Diabetic kidney disease; renal tubular epithelial cells; CD36; mitochondrial function; fatty acid oxidation


1. Introduction


Diabetic kidney disease (DKD) is the most common cause of kidney failure worldwide, affecting approximately 40% of patients with diabetes [1]. Much progress has been made over the past few decades to understand the pathophysiology of DKD. Nevertheless, current therapeutic regimens can slow down but not stop or reverse disease progression, highlighting the urgency of exploring the underlying mechanisms [1]. The primary pathological changes in DKD include glomerular lesions, particularly mesangial expansion, and glomerular basement membrane thickening [2]. Recent evidence indicates that tubulointerstitial injury is a critical predictor of the progression of DKD to end-stage renal disease [2,3]. In fact, some studies have reported the extent of tubular injury in DKD, also known as diabetic tubulopathy [3]. Therefore, identifying novel molecular targets of diabetic tubular injury appears to be a promising strategy for treating DKD.

Mitochondria, the powerhouses of the cell, produce ATP *via* oxidative phosphorylation and fatty acid oxidation (FAO). The kidney is a high-energy demand organ, and kidney and mitochondrial functions are closely associated [4]. Mitochondrial dysfunction plays a vital role in the pathogenesis and development of various kidney diseases [5–7]. In the

last few years, studies involving animal models and patients with diabetes have reported that improving mitochondrial function is beneficial for recovery from kidney diseases [8]. Proximal tubules utilize the majority of oxygen for ATP generation to enable the reabsorption of metabolites and contain the highest number of mitochondria in the kidney. Mitochondrial FAO is the preferred source of ATP in renal tubular epithelial cells (TECs). Defects in FAO play a key pathogenic role in tubulointerstitial fibrosis. Restoring fatty acid metabolism using genetic or pharmacological methods has been found to prevent renal fibrosis progression [9,10]. Furthermore, recent omics studies have provided unbiased evidence that both mitochondrial dysfunction and impaired renal tubular FAO play pivotal roles in DKD development [11]. In our previous study, we found that high glucose-induced HK-2 cells and mouse models with DKD displayed lower expression of key enzymes and regulators of FAO and higher levels of injured tubular cells [12,13]. However, the detailed molecular mechanisms underlying impaired FAO in diabetic TECs remain elusive.

CD36, a fatty acid transporter protein, is a single-chain transmembrane surface glycoprotein that belongs to the class B scavenger receptor family [14]. CD36 is highly

CONTACT Lihua Wang  lihuawang236@126.com  Department of Nephrology, Second Hospital, Shanxi Medical University, No.382, Wuyi Road, Taiyuan, Shanxi Province 030000, China.

 Supplemental data for this article can be accessed online at <https://doi.org/10.1080/0886022X.2023.2292753>.

© 2023 The Author(s). Published by Informa UK Limited, trading as Taylor & Francis Group
This is an Open Access article distributed under the terms of the Creative Commons Attribution-NonCommercial License (<http://creativecommons.org/licenses/by-nc/4.0/>), which permits unrestricted non-commercial use, distribution, and reproduction in any medium, provided the original work is properly cited. The terms on which this article has been published allow the posting of the Accepted Manuscript in a repository by the author(s) or with their consent.

abundant in proximal tubular cells [15], and antagonist blockade or genetic knockout of CD36 contributes to alleviate tubulointerstitial inflammation and fibrosis [16]. CD36 exerts these biological effects *via* a signaling receptor that responds to innate immune reactions and a long-chain free fatty acid transporter, leading to intracellular lipid accumulation [15]. Recently, an association between CD36 and mitochondrial FAO has been reported. A study found that CD36 expression in cardiac myocytes inhibited AMPK activation, consequently affecting AMPK-mediated FAO [17]. The significance of CD36 in FAO is related to its function in the mitochondrial transfer of fatty acids, as previously demonstrated in human skeletal muscle cells [18] and macrophages [16]. Furthermore, inhibition of CD36 palmitoylation enhances hepatic FAO by interacting with long-chain acyl-CoA synthetase-1 [19]. In our previous study, we confirmed that the downregulation of CD36 expression contributes to the upregulation of FAO-related enzymes and AMPK activity in the kidneys of db/db mice [12]. We believe that CD36 deletion regulates FAO activation and contributes to improved mitochondrial function in diabetic TECs.

In this study, we found that CD36 deletion reduced the progression of diabetic nephropathy, improved mitochondrial dysfunction, and enhanced FAO-associated mitochondrial respiration in diabetic TECs. Furthermore, we observed that the pyruvate dehydrogenase kinase-4 (PDK4)-AMPK axis plays an essential role in downregulating the expression of functional genes involved in fatty acid metabolism. Taken together, our data indicate that CD36 inhibition can serve as a potential therapeutic strategy to improve mitochondrial function and restore FAO in patients with DKD.

2. Materials and methods

2.1. Experimental animals

Eight-week-old CD36 knockout (CD36KO, C57BLKS/J background, $n=12$) mice were obtained from GemPharmatech Co., Ltd. The results of the identification of the CD36 knockout were provided by GemPharmatech Co., Ltd. and validated in this study (Supplementary Figure 1A). Wild-type (WT, $n=12$) littermates were used as controls. All the animals had the same genetic background. Half of the WT and CD36KO mice were injected with streptozotocin (STZ) and a high-fat diet (establishment of a diabetic model), as previously described [13]; the other half of the WT and CD36KO mice were administered citrate buffer and used as controls. Mice in the diabetic model group (DM) had *ad libitum* access to a high-fat diet (#D12492), whereas those in the WT group ($n=6$) and CD36KO group ($n=6$) were fed standard rodent chow. After 4 weeks, mice in the diabetic model group were intraperitoneally injected with STZ (50 mg/kg STZ in fresh 0.1 M sodium citrate buffer, pH 4.5) daily for 5 days, and those in the WT group were administered citrate buffer. One week later, mice with blood glucose levels >11.1 mmol/L were identified and used for further analyses (i.e., successful models). All animals were housed in a temperature-controlled

room at the Animal Center of Shanxi Medical University with a 12-h light/dark cycle and had *ad libitum* access to food and water. At the end of the experiment, all animals were anesthetized and sacrificed after 12 h of fasting at 24 weeks of age. Blood samples, 24-h urine samples, and kidney tissues were collected from each animal for further analysis. All experimental protocols were conducted in accordance with the Ethics Review Committee for Animal Experimentation of Shanxi Medical University.

2.2. Biochemical analyses

Blood samples were collected from the retroorbital plexus and centrifuged at 3000 rpm for 15 min to obtain serum samples. Blood glucose, blood creatinine, and blood urea nitrogen concentrations were determined in serum samples using a biochemical autoanalyzer (Lanyun, Shenzhen, China), as to standard laboratory procedures. All procedures were performed in accordance with the manufacturer's instructions. Urine was collected over a 24-h period, during which each animal was placed in an individual metabolic cage. Urinary albumin levels were measured using reagent kits (BioSino Bio-Technology and Science Inc., Beijing, China), according to the manufacturer's instructions. The 24-h urinary albumin excretion rate was determined using the following formula: urinary albumin ($\mu\text{g/mL}$) \times 24-h urine volume (mL).

2.3. Renal pathology and immunohistochemistry

Renal tissues were fixed in 4% paraformaldehyde overnight at 4°C, dehydrated, embedded in paraffin, 4 μm -thick tissue sections were prepared for histopathological analysis. Periodic acid-Schiff (PAS) staining was performed, as previously described [8], to evaluate tubular injury. Briefly, 30 glomeruli and approximately 80 ± 100 proximal tubules from each mouse (8 mice/group) were semiquantitatively analyzed using the ImageJ image processing and analysis system. Quantification of the glomerular volume and proximal tubular area was conducted by a pathologist in a blinded manner. The percentage of damaged tubules (interstitial inflammation and fibrosis, tubular dilation, and cast formation) was graded from 0 to 3 as follows: -0, normal; 1, tubular lesion $< 25\%$; 2, 25%–50% tubular lesion; and 3, tubular lesion $> 50\%$. Immunohistochemistry of renal sections was performed using the SP kit, according to the manufacturer's instructions [11]. Labeling was visualized with 3,3'-diaminobenzidine to produce a brown color, and the sections were counterstained with hematoxylin. All corresponding antibodies are listed in Supplementary Table 1. The staining results were analyzed using light microscopy by two independent, blinded observers. The images thus obtained were assessed using ImageJ software (National Institutes of Health). Mitochondrial morphology was assessed by transmission electron microscopy. Briefly, small cubes of renal cortex tissues were fixed in 2.5% glutaraldehyde for 24 h at 4°C, and mitochondria were assessed by the Kingmed Medical Test Center (Taiyuan,

China). Sections were examined and photographed using a transmission electron microscope (Hitachi, Tokyo, Japan). ImageJ was used to measure the peripheral glomerular basement membrane length, as previously described [12].

2.4. Terminal deoxynucleotidyl TUNEL staining

Kidney cell apoptosis was evaluated using the TUNEL FITC Apoptosis Detection Kit (Promega Corp., Madison, WI, USA), according to the manufacturer's instructions. To quantify apoptotic cells, at least 500 cells were counted per well, and the percentage of positively labeled cells was calculated.

2.5. Measurement of mitochondrial DNA (mtDNA) content

The mtDNA copy number was quantified by RT-PCR using a Mouse mtDNA Copy Number Assay Kit (MCN3; Detroit R&D, Detroit, MI, USA), according to the manufacturer's instructions. Total DNA was extracted from renal cortical tissue. Reactions were performed using 10 ng of DNA. The relative mtDNA copy number was presented as the ratio of mtDNA to nuclear DNA.

2.6. Mouse primary renal tubular cell culture and measurement of viability

Mouse primary renal tubular cells were isolated from WT, WT+DM, CD36KO, and CD36KO+DM mice using a previously reported method [12]. Briefly, renal cortex tissue was dissected, placed in ice-cold Dulbecco's PBS (DPBS) and minced into pieces. Fragments were transferred to a 50 mL tube containing 10 mL of DMEM medium with 100 μ L of Collagenase I and digested for 30 min at 37°C in a 160/170 rpm shaker. Thereafter, 100 μ L of FBS (Thermo Fisher Scientific) was added to stop the Collagenase I reaction. Cells were further sieved through a 100 μ m nylon mesh, followed by 70 μ m and 40 μ m nylon meshes. Cells were centrifuged for 10 min at 3000g. The pellet was resuspended in 1 mL of sterile RBC lysis buffer and incubated for 2–3 min on ice. DPBS was added, followed by centrifugation for 10 min at 3000g. The cells were cultured in DMEM supplemented with 10% fetal bovine serum (Gibco, 16000–044) and 1% penicillin and streptomycin (Gibco, 15140–122) at 37°C and 5% CO₂. TECs were identified by immunofluorescence staining for cytokeratin-18 (Supplementary Figure 1B). Images were obtained using an Olympus CKX41 inverted microscope (Tokyo, Japan).

2.7. Measurement of oxygen consumption rate (OCR)

Mouse primary renal TECs were seeded in a specialized XF24 cell culture microplate (Seahorse Bioscience) at a density of 50,000–80,000 cells/well. These cells were exposed to different experimental conditions, and OCR was measured using a Seahorse Bioscience Extracellular Flux Analyzer (Agilent). After cell lysis in radioimmunoprecipitation assay (RIPA) buffer, a protein assay was performed. OCR values were normalized to the protein content of each well.

2.8. In situ enzyme staining of cytochrome c oxidase

In situ enzyme staining for cytochrome c oxidase was performed as previously described [6,7]. Briefly, mouse kidneys were immediately frozen in isopentane (JUNSEI, Japan) cooled with liquid nitrogen, cryosected (12 μ m), and incubated with cytochrome c oxidase reaction solution (Sigma-Aldrich) for 30 min at room temperature. Images were obtained using an Olympus BX53 upright microscope and quantified using the ImageJ software.

2.9. Intracellular ATP level measurement

Intracellular ATP content in primary renal epithelial cells was measured using the ATP Colorimetric/Fluorometric Assay Kit (BioVision Inc., Milpitas, CA, USA), according to the manufacturer's instructions. The data was normalized to the total protein content.

2.10. Intracellular cAMP level measurement

Intracellular cAMP levels in primary tubular cells were determined using an ABI (T1500), according to the manufacturer's instructions.

2.11. Western blotting

Proteins were extracted from renal cortex tissues using RIPA buffer, separated by SDS-PAGE, and transferred to a polyvinylidene difluoride membrane (Millipore, Billerica, MA, USA). The membrane was then incubated with specific primary antibodies (Supplementary Table 1) overnight at 4°C, followed by incubation with goat anti-rabbit or mouse IgG horseradish peroxidase conjugate (1:10,000 dilution, Santa Cruz, CA, USA). Immunoblots were visualized using the ECL detection system and scanned using the ChemiDoc™ Imaging System (Bio-Rad, USA).

2.12. Quantitative RT-PCR

Total RNA and cDNA were obtained from frozen renal cortex tissues using TRIzol (Invitrogen) and RT-qPCR kits (Thermo Fisher Scientific), according to the manufacturer's instructions. Quantitative RT-PCR was performed using SYBR Premix Ex Taq (Takara Bio Inc.) on an Agilent Mx3000P qPCR System (Agilent, Palo Alto, CA, USA). Normalization was performed using 18S rRNA. Primer sequences used for mRNA quantification are listed in Supplemental Table 2.

2.13. Statistical analysis

Values represent the mean \pm SD. Differences between groups were analyzed for statistical significance using one-way analysis of variance (ANOVA), followed by a post-hoc test using the Tukey–Kramer method. All experiments were performed at least thrice. Statistical significance was set at $p < 0.05$.

3. Results

3.1. CD36 deletion ameliorates renal injury in diabetic mice

To investigate the role of CD36 in the pathogenesis of renal injury in diabetic nephropathy, we induced type 2 diabetes in CD36^{+/+} (WT) and CD36^{-/-} (KO) mice for 24 weeks. The level of CD36 expression were significantly inhibited in CD36^{-/-} (KO) mice (Figure 1(A) and Figure 4(E)). CD36^{-/-} (KO) mice showed no significant phenotypic changes compared with the CD36^{+/+} (WT) mice. Then, we assessed biochemical indices of renal function. Compared with WT mice, diabetic mice showed a significant increase in blood creatinine and blood urea nitrogen levels. CD36 deletion significantly ameliorated this abnormal increase in blood creatinine and urea nitrogen levels in diabetic mice, implying that CD36 aggravates renal function (Table 1). Diabetic mice also showed a significant increase in blood glucose and 24-h urinary albumin levels and kidney weight-to-body weight ratio; CD36 deletion restored these changes (Table 1). Periodic acid-Schiff staining revealed renal glomerular basement membrane thickening and mesangial matrix proliferation (Figure 1(A)). Transmission electron microscopy revealed significant ultrastructural changes in diabetic mice, including fusion of foot processes and thickening of the glomerular basement membrane (Figure 1(A,B)). These changes were alleviated in CD36KO mice with diabetes, as indicated by the glomerular damage and tubulointerstitial damage scores (Figure 1(C,D)). We also examined extracellular matrix expression and renal fibrotic lesions. Compared to the WT group, collagen I and fibronectin expression levels were significantly upregulated in the diabetic WT group, and these changes were significantly reduced in CD36KO mice (Figure 1(A,E)). Moreover, the number of TUNEL-positive cells in the kidneys of diabetic CD36KO mice was lower than that in the kidneys of WT mice (Figure 1(F,G)). Western blotting was used to determine the expression levels of apoptosis-associated proteins. Relative to the WT group, the Bax/Bcl-2 ratio and cleaved caspase-3 expression showed a considerable increase in the diabetic group; these values were lower in the CD36KO mice with diabetes (Figure 1(H)). Collectively, these data suggest that CD36 plays a vital role in inducing renal injury in diabetic mice.

3.2. CD36 deletion improves mitochondrial injury and dysfunction in the kidney of diabetic mice

Mitochondrial dysfunction, associated with changes in mitochondrial morphology, is an important feature of diabetic renal injury [5]. Oxidized LDL/CD36 signaling in macrophages contributes to mitochondrial metabolic reprogramming [8]. Thus, we evaluated the morphological alterations of mitochondria in renal cortical tissue using transmission electron microscopy. Cells from tubular segments within the kidneys of WT mice showed regular apical microvilli, intact basement membranes, and basal infoldings (Figure 2(A)). Mitochondria in these cells were abundant, appeared elongated, and

showed a good cristina in the inner matrix. In contrast, most diabetic kidney cells seemed to have lost mitochondrial cristae, with fragmented, small, and round mitochondria. CD36 deletion significantly improved most of these morphological alterations in mitochondria (Figure 2(B)), and the reduction in mitochondrial mass induced by diabetes was almost abrogated in the renal TECs of diabetic mice (Figure 2(C)). Furthermore, to investigate the effects of CD36 on mitochondrial function in diabetic kidneys, we examined the OCR of isolated primary renal tubular cells from WT, WT+DM, CD36KO, and CD36KO+DM mice using an XF24 Flux Analyzer. OCR showed a considerable decrease in diabetic primary renal tubular cells, which was partially restored in diabetic CD36KO mice (Figure 2(D)). The decrease in ATP levels in diabetic primary renal tubular cells was also preserved in CD36KO mice (Figure 2(E)). Western blotting indicated that the proteins levels of mitochondrial electron transport chain complexes, most notably I, III, and IV, were upregulated in the kidneys of diabetic CD36KO mice compared to those of diabetic WT mice (Figure 2(F)). Moreover, we observed a reduction in cytochrome c oxidase activity in the kidneys of diabetic WT mice, a hallmark of mitochondrial damage, which was preserved in the kidneys of diabetic CD36KO mice (Figure 2(G,H)). Collectively, these findings suggest that increased mitochondrial dysfunction in the kidney of diabetic mice was markedly reversed by CD36 deletion.

3.3. CD36 deletion prevents impairment of FAO-associated respiration in diabetic TECs

Considering that kidney tubule segments are enriched with mitochondria and that mitochondrial FAO is a major contributor to intracellular ATP production in TECs [5], we investigated whether the protective effects of CD36 deletion on diabetic kidney are related to preventing FAO impairment. First, we determined the gene expression levels of PPAR α , a key transcription factor that regulates mitochondrial FAO pathways, in the kidneys of each study group. The mRNA level of PPAR α was markedly downregulated in diabetic mice; compared to that in WT mice, and was upregulated in diabetic CD36KO mice (Figure 3(A)). We also evaluated the expression levels of well-known PPAR α target genes by RT-PCR. The expression levels of most PPAR α target genes (Cpt1a, Acox1, Lcad, Mcad, Acad10, and Hadh) tended to be downregulated in diabetic WT mice, and this effect was reversed in diabetic CD36KO mice (Figure 3(A)). We further examined the protein expression levels of CPT1a and ACOX1, which are the key rate-limiting enzymes in FAO. Relative to the kidneys of non-diabetic WT mice, diabetic WT mice showed significantly downregulated CPT1a and ACOX1 protein expression levels; CD36 deletion upregulated these levels (Figure 3(B)). The decreased levels of PPAR α and its target protein ACOX1 were further verified by immunohistochemistry (Figure 3(C)). PPAR α and ACOX1 are primarily localized in tubular epithelial regions. Taken together, these findings suggest that CD36 deletion prevents the impairment of FAO-associated respiration in diabetic TECs.

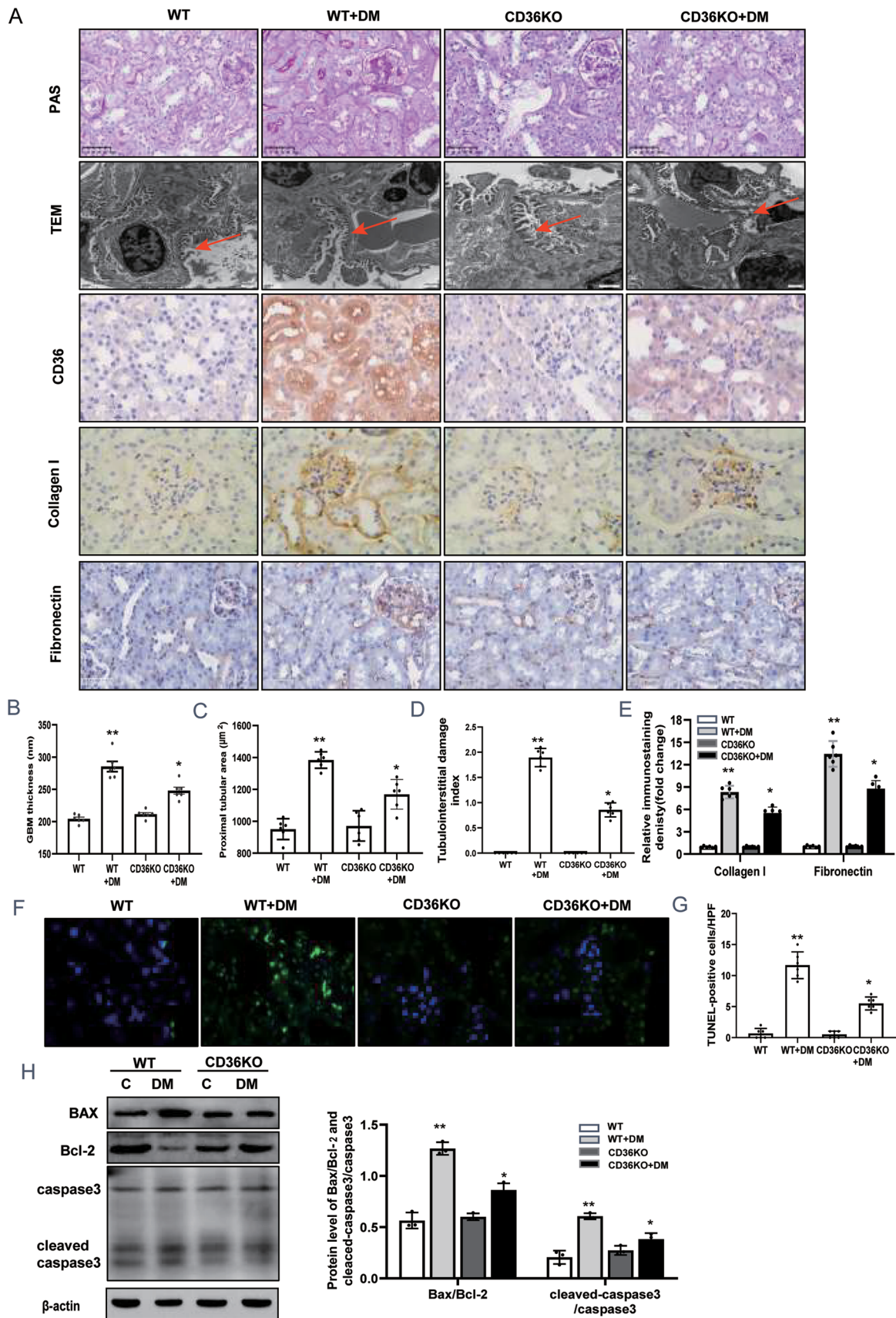


Figure 1. Deletion of CD36 ameliorates renal injury in diabetic mice. (A) Kidney sections were stained with periodic acid Schiff, transmission electron microscopy and immunohistochemical staining images (Bar 50µm). The GBM thickness (B), proximal tubular area (C) and tubular interstitial damage scores (D) were measured. (E) Semi-quantitative analysis of Fibronectin and Collagen I from immunohistochemical staining data (8–10 sections per mouse were analyzed). (F) Apoptosis was assessed by TUNEL (Bar = 50µm). (G) Apoptotic cells per field. (H) The expression levels of cleaved caspase-3, Bax, and Bcl-2 were detected by Western blot analysis. Data are expressed as mean±SD. (n=6). ***p* < .01 vs WT group, **p* < .05 vs WT+DM group.

Table 1. Change of basic parameters in each group.

Group	BG (mmol·L ⁻¹)	Scr (μmol·L ⁻¹)	BUN (mmol·L ⁻¹)	UAE (μg·24 h ⁻¹)	KW/BW (mg/g)
WT	5.62 ± 0.32	11.29 ± 3.45	11.22 ± 2.23	5.12 ± 1.12	4.01 ± 0.98
WT + DM	19.76 ± 3.91*	28.32 ± 4.01*	23.98 ± 8.57	291.65 ± 11.23*	6.01 ± 1.03*
CD36KO	4.91 ± 1.02 [#]	6.15 ± 4.07*	7.52 ± 3.89	4.89 ± 2.53*	4.01 ± 0.21*
CD36KO + DM	7.91 ± 4.32*	17.21 ± 2.54 [#]	15.32 ± 4.52	211.46 ± 16.23 [#]	5.23 ± 0.84 [#]

Date are presented as the mean ± SD (*n* = 6). BG: blood glucose; Scr: serum creatinine; BUN: blood urea nitrogen; UAE: urine albumin excretion; KW/BW: kidney weight/body weight.

**p* < .05 versus WT; [#]*p* < .05 versus WT + DM.

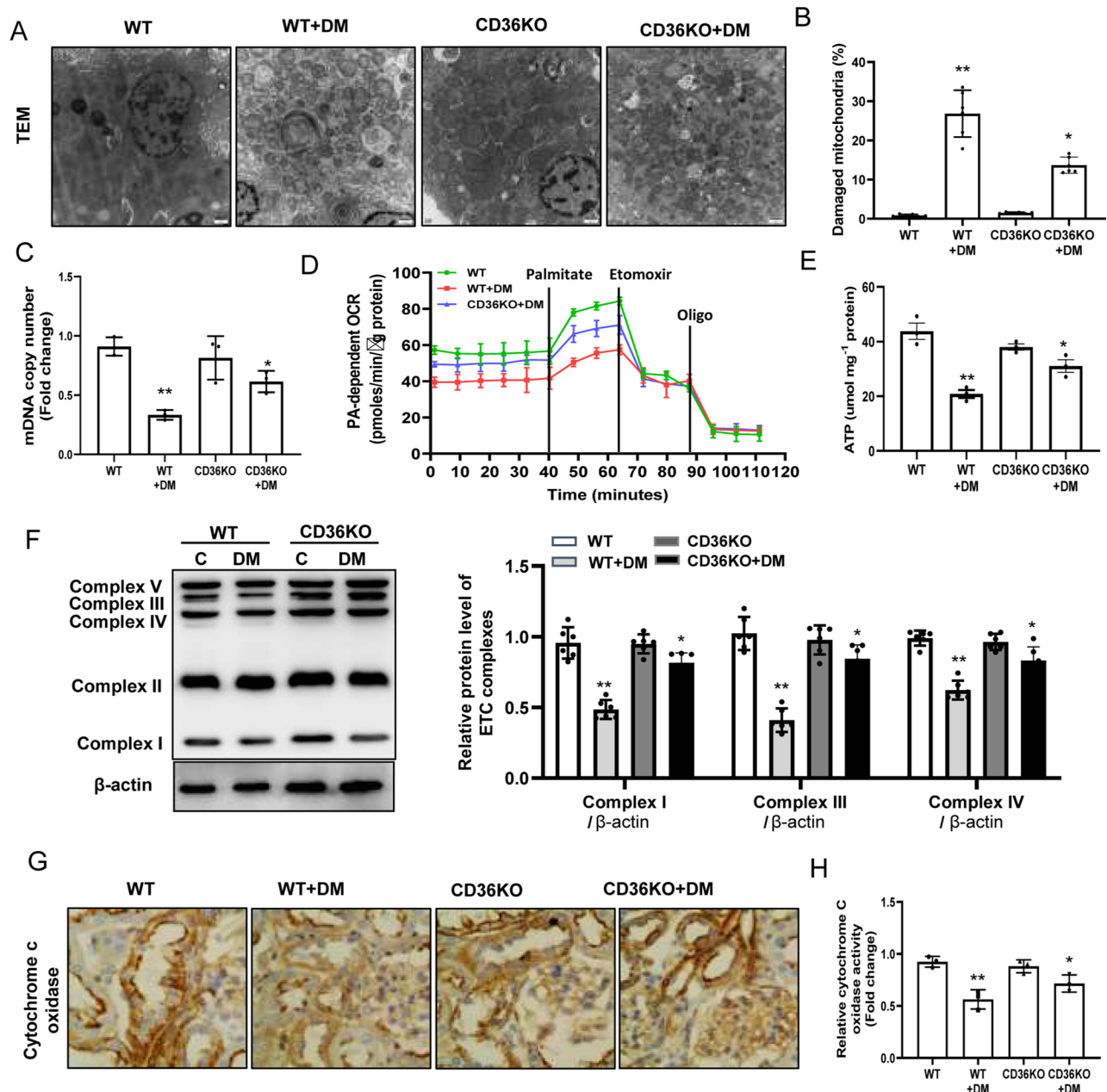


Figure 2. Deletion of CD36 improves mitochondrial injury and dysfunction in kidney of diabetic mice. (A) Representative transmission electron microscopy micrographs for mitochondria. Quantification analysis of average damaged mitochondria (B) and mDNA copy number (C). (D) Oxygen consumption rate (OCR) of TECs measured with a Seahorse XF24 Extracellular Flux Analyzer. (E) ATP levels of TECs from each group. (F) Representative Western blot and analysis for the expression of Complex I, Complex IV, and Complex V in kidney tissues. (G) Representative images and analysis (H) of Cytochrome c oxidase in kidney sections. Data are expressed as mean ± SD. (*n* = 6). ***p* < .01 vs WT group, **p* < .05 vs WT + DM group.

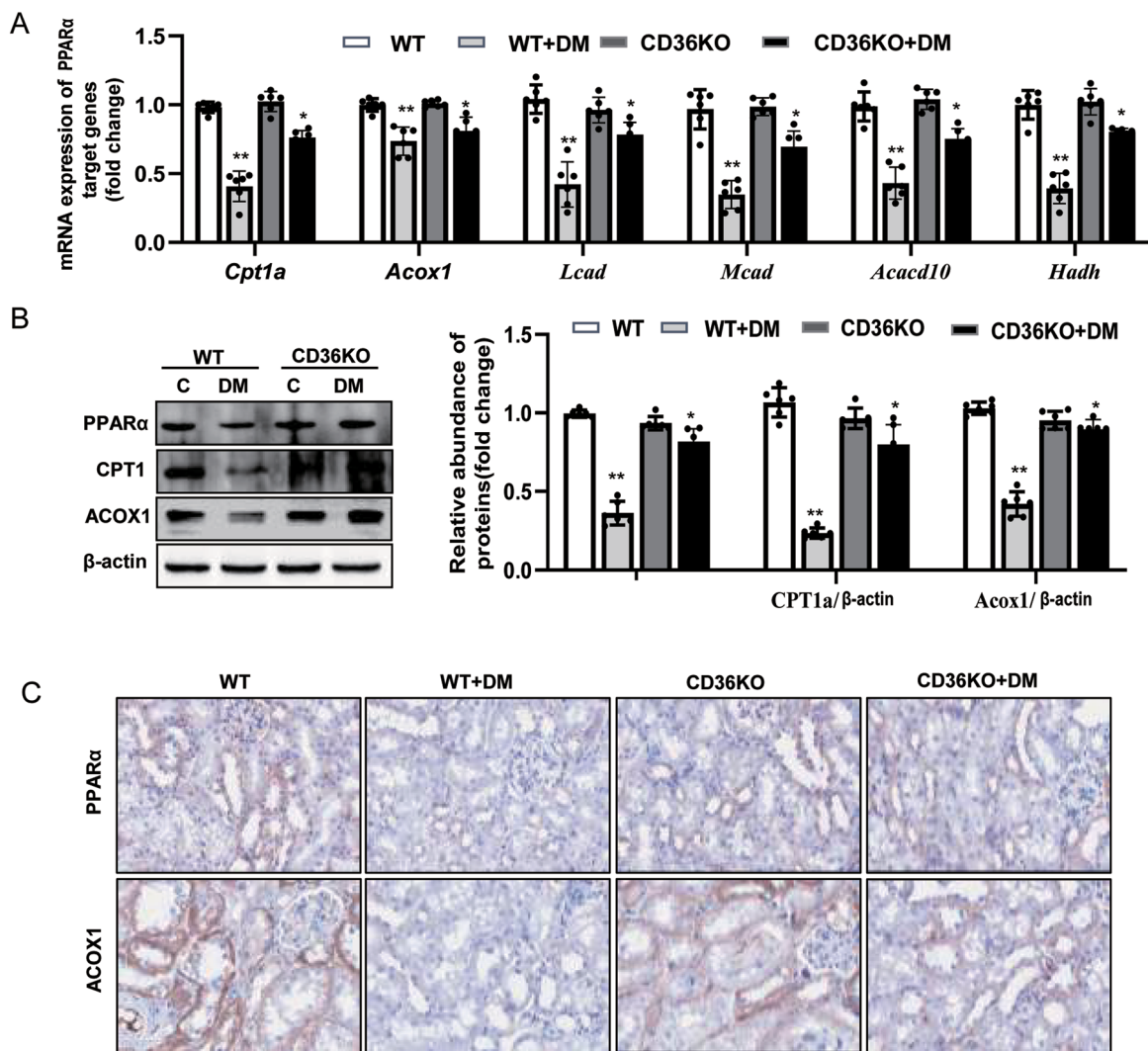


Figure 3. Deletion of CD36 prevents impairment of FAO-associated respiration in diabetic TECs. (A) The mRNA levels of *ppara*, *cpt1a*, *acox1*, *lcad*, *mcad*, *acacd10*, and *hadh* was analyzed by RT-qPCR. (B). Representative Western blot and analysis for the expression of PPARα, Cpt1A, and ACOX1. (C). Representative images of immunohistochemical staining of PPARα, and ACOX1. (Bar = 50 μm). Data are expressed as mean ± SD. (n=6). ***p* < .01 vs WT group, **p* < .05 vs WT+DM group.

3.4. CD36 regulates mitochondrial energy metabolism through PDK4-AMPK axis inactivation in diabetic TECs

PDK4 is an important mitochondrial matrix enzyme involved in cellular energy regulation in tissues with high energy demands [5]. PDK4 mRNA is a sensitive marker of FAO [5]. Therefore, we verified the association between CD36 and the PDK4-AMPK signaling pathways in diabetic TECs. We observed an approximately 63% decrease in PDK4 mRNA levels (Figure 4(A)) and an approximately 89% decrease in PDK4 protein expression levels (Figure 4(E)) in diabetic mice compared to those in WT mice. CD36 deletion restored the reduction in PDK4 mRNA and protein expression levels (approximately 98% increase). Immunofluorescent staining and quantitative data showed that CD36 levels increased in the areas with high levels of KIM1, a marker of tubular injury (Figure 4(B)). Negative correlations were observed between tubular interstitial damage and PDK4 ($r = -0.75$) (Figure 4(C)) and between PDK4 and KIM1 levels ($r = -0.69$) (Figure 4(D)) in

the kidney tissues of diabetic mice. PDK4 plays a critical role in regulating cAMP levels. Consistent with the increase in PDK4 expression levels upon CD36 deletion, primary renal tubular cells from CD36KO mice showed a decrease in cAMP levels (Figure 4(F)) and an increase in AMPK phosphorylation (Figure 4(E)), consistent with the results of our previous study [5]. These data suggest that CD36 alters mitochondrial metabolic pathways improve diabetic renal tubular injury, partly through the inactivation of the PDK4-AMPK axis at the transcriptional level.

4. Discussion

The transmembrane protein CD36 plays an important role in various forms of kidney diseases. The main mechanisms reported so far have focused on the effects of CD36 on intracellular lipid deposition and CD36-mediated innate immunity. Our findings demonstrated that CD36 contributes to

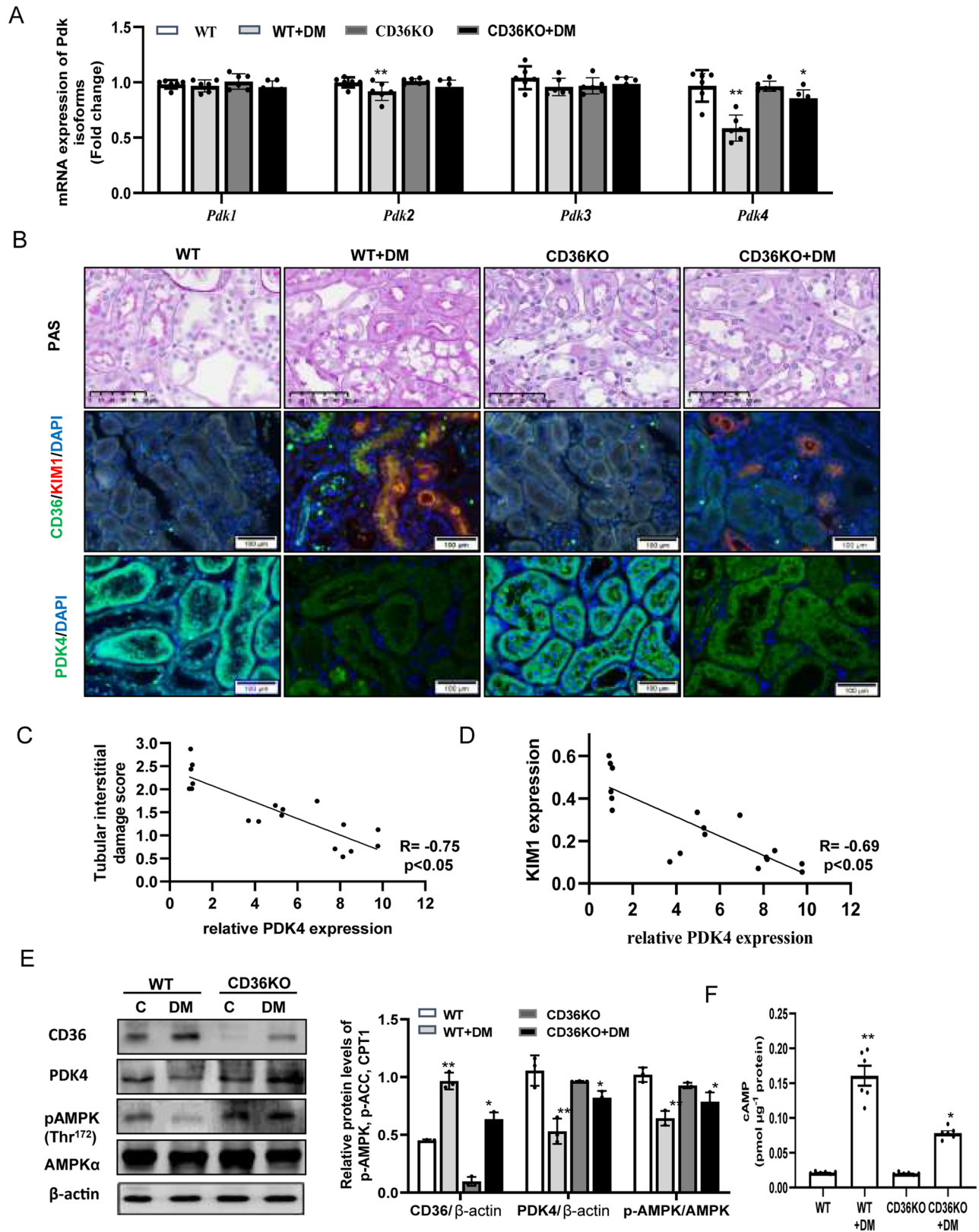


Figure 4. CD36 regulates mitochondrial energy metabolism through inactivated PDK4-AMPK axis in diabetic kidney. (A) The mRNA levels of *Pdk1*, *Pdk2*, *Pdk3*, and *Pdk4* was analyzed by RT-qPCR. (B) Kidney sections were stained with periodic acid Schiff (Bar 50 μm). Representative images of CD36/KIM1 immunofluorescence Co-staining labeling in kidney tissue. Positive staining is yellow. Representative images of PDK4 immunofluorescence labeling in kidney tissue. Positive staining is green. Tubular interstitial damage scores (C) and KIM1 expression were measured (D). (E) Representative Western blot and analysis for the expression of CD36, PDK4, P-AMPK, and AMPK. (F) cAMP levels in total kidney tissue. Data are expressed as mean ± SD. (n=6). **p < .01 vs WT group, *p < .05 vs WT+DM group.

diabetes-induced-mitochondrial damage and FAO impairment in TECs. Mechanistically, we found that the relationship between CD36 and mitochondrial function seemed to be partially related to the activity of the PDK4–AMPK axis. Thus, our results highlight a novel mechanism underlying mitochondrial dysfunction in diabetic kidney.

In recent years, with the emergence of the ‘tubular centric view of DKD’ [20], FAO impairment in TECs and mitochondrial damage in the pathogenesis of DKD have received increased attention [2,20]. In DKD, both pharmaceutical mitochondrial protection and genetic intervention to improve mitochondrial function have strong renoprotective effects [16]. Furthermore, diabetic kidney drugs improve mitochondrial function and energy supply in renal tubular cells [21]. Renal tubular cells are the most abundant in the mitochondria, and mitochondrial FAO is the preferred source of energy for these cells. Mitochondrial FAO impairment is an important mechanism underlying tubular injury in chronic kidney diseases, including diabetes mellitus. Further studies are warranted to explore these underlying mechanisms.

CD36 is a cell membrane transporter that is expressed on the surface of many cell types [15]. It serves as a receptor for many endogenous ligands, and plays various roles in the regulation of physiological and pathological functions. The role of CD36 in the kidney has been extensively investigated [15]. In experimental models, antagonist blockade or genetic knockout of CD36 was found to prevent kidney injury, demonstrating its potential as a therapeutic target for chronic kidney disease [15]. In addition, Suszak et al. first reported in 2016 that CD36 is expressed in diabetic renal tubules and mediates TEC apoptosis [22]. Follow-up studies suggest that CD36 serves as a signaling hub for lipid homeostasis and immunological responses [8]. CD36 also regulates mitochondrial FAO and promotes macrophage activation [8]. It localizes to the mitochondria and regulates lipid metabolism in skeletal muscle cells and cardiomyocytes [23]. However, no direct evidence has highlighted the effects of CD36 on mitochondrial damage in DKD patients. In this study, we found that CD36 deletion improved renal function and morphopathological changes in diabetic mice, which is consistent with the results of a previous study. We also observed a significant improvement in the mitochondrial morphology of the renal tubular cells. Thus, we investigated the effects of CD36 on the protein levels of mitochondrial electron transport chain complexes and on the synthesis of ATP in mouse primary renal tubular cells and found that mice with DKD showed a decrease in the expression levels of oxidative phosphorylation proteins and synthesis of ATP; CD36 knockout reversed this effect. Because fatty acids are the preferred energy source for proximal tubular cells, a reduction in FAO in DKD plays an important role in the pathogenesis of kidney fibrosis. Furthermore, we found that CD36 knockout upregulated the expression of key FAO enzymes. These data indicate that CD36 knockout promotes mitochondrial energy metabolism and that diabetes-induced CD36 expression is involved in renal tubular energy disturbance.

In terms of the mechanisms by which CD36 mediates mitochondrial energy metabolism, we focused on elucidating its effects on PDK4 expression. PDKs act as tissue homeostats to support adequate context-dependent regulation of energy-fueling pathways [5]. PDK4 is a key mitochondrial matrix enzyme involved in cellular energy regulation in tissues with high energy demands. In the kidney, it is the main isoform of PDKs and is involved in lipid-related metabolic adaptations under various disease conditions [24]. The upregulation of PDK4 expression indicates a metabolic shift toward the increased utilization of fatty acids as an energy fuel [5]. Therefore, PDK4 is considered a sensitive marker for increased FAO [5]. We found that the mRNA and protein expression levels of PDK2/4 were markedly downregulated in the renal cortex tissues of diabetic mice, whereas those of other PDK isoforms (PDK1/3) remained unchanged. Increased CD36 expression could reduce the expression of PDK4 in diabetes induced muscle cells [19]. We also found that the CD36 knockout upregulated PDK4 expression. CD36 thus seems to mediate PDK4 inactivation in DKD patients. Zhou et al. [25] found that PDK4 was mainly expressed in proximal TECs and that its expression was downregulated in chronic kidney disease, with decreased energy metabolism. Oh et al. [25] demonstrated the involvement of PDK4 in cisplatin-induced acute kidney injury, intervention with a PDK inhibitor, and knockout of PDK4. Increased levels of PDK4 have been previously found to inhibit the pyruvate dehydrogenase complex (PDH), and phosphorylation of PDHE1a, a target protein of PDK4, thereby leading to an influential metabolic shift from glycolysis to FAO [26]. Our results indicate that PDK4 activation was significantly inhibited in diabetic kidneys, but PDHE1a mRNA expression levels did not show a significant change. Compared with the normal group, the diabetic renal cortex showed an approximately 89% decrease in PDHE1 phosphorylation at the protein expression level; CD36 knockout did not affect this. Altered ATP production by FAO in response to PDK4 expression is responsible for changes in AMP levels [27], with CD36 being a negative regulator of AMPK activation [17]. Our data confirmed that CD36 deletion increases AMPK. However, further studies are warranted to determine how PDK4 directly responds to changes in CD36 in DKD. Our results suggest that CD36 alters cellular metabolic pathways in diabetic kidneys partly through inactivation of the PDK4–AMPK axis at the transcriptional level.

In summary, we report key evidence indicating that diabetes-induced upregulation of CD36 in TECs contributes to the pathogenesis of DKD by restoring FAO and improving mitochondrial function. This study highlights CD36 as a regulator of cellular energy metabolism and a potential target for the future development of promising therapeutic strategies.

Acknowledgements

We would like to thank the native English-speaking scientists of the Elixigen Company (Huntington Beach, California) for editing our manuscript.

Disclosure statement

No potential conflict of interest was reported by the author(s).

Funding

This work was supported by a grant from the National Natural Science Foundation of China [grant number: 81900670].

Data accessibility statement

The data used in the study can be made available by the corresponding author upon reasonable request.

References

- [1] Alicic RZ, Rooney MT, Tuttle KR. Diabetic kidney disease: challenges, progress, and possibilities. *Clin J Am Soc Nephrol.* 2017;12(12):2032–2045. doi: [10.2215/CJN.11491116](https://doi.org/10.2215/CJN.11491116).
- [2] Higgins GC, Coughlan MT. Mitochondrial dysfunction and mitophagy: the beginning and end to diabetic nephropathy? *Br J Pharmacol.* 2014;171(8):1917–1942. doi: [10.1111/bph.12503](https://doi.org/10.1111/bph.12503).
- [3] Zeni L, Norden AGW, Cancarini G, et al. A more tubulocentric view of diabetic kidney disease. *J Nephrol.* 2017;30(6):701–717. doi: [10.1007/s40620-017-0423-9](https://doi.org/10.1007/s40620-017-0423-9).
- [4] Bhargava P, Schnellmann RG. Mitochondrial energetics in the kidney. *Nat Rev Nephrol.* 2017;13(10):629–646. doi: [10.1038/nrneph.2017.107](https://doi.org/10.1038/nrneph.2017.107).
- [5] Pettersen IK, Tusubira D, Ashrafi H, et al. Upregulated PDK4 expression is a sensitive marker of increased fatty acid oxidation. *Mitochondrion.* 2019;49:97–110. doi: [10.1016/j.mito.2019.07.009](https://doi.org/10.1016/j.mito.2019.07.009).
- [6] Wei PZ, Szeto CC. Mitochondrial dysfunction in diabetic kidney disease. *Clin Chim Acta.* 2019;496:108–116. doi: [10.1016/j.cca.2019.07.005](https://doi.org/10.1016/j.cca.2019.07.005).
- [7] Tang C, Cai J, Yin XM, et al. Mitochondrial quality control in kidney injury and repair. *Nat Rev Nephrol.* 2021;17(5):299–318. doi: [10.1038/s41581-020-00369-0](https://doi.org/10.1038/s41581-020-00369-0).
- [8] Chen Y, Yang M, Huang W, et al. Mitochondrial metabolic reprogramming by CD36 signaling drives macrophage inflammatory responses. *Circ Res.* 2019;125(12):1087–1102. doi: [10.1161/CIRCRESAHA.119.315833](https://doi.org/10.1161/CIRCRESAHA.119.315833).
- [9] Kang HM, Ahn SH, Choi P, et al. Defective fatty acid oxidation in renal tubular epithelial cells has a key role in kidney fibrosis development. *Nat Med.* 2015;21(1):37–46. doi: [10.1038/nm.3762](https://doi.org/10.1038/nm.3762).
- [10] Chung KW, Lee EK, Lee MK, et al. Impairment of PPAR α and the fatty acid oxidation pathway aggravates renal fibrosis during aging. *J Am Soc Nephrol.* 2018;29(4):1223–1237. doi: [10.1681/ASN.2017070802](https://doi.org/10.1681/ASN.2017070802).
- [11] Hou Y, Shi Y, Han B, et al. The antioxidant peptide SS31 prevents oxidative stress, downregulates CD36 and improves renal function in diabetic nephropathy. *Nephrol Dial Transplant.* 2018;33(11):1908–1918. doi: [10.1093/ndt/gfy021](https://doi.org/10.1093/ndt/gfy021).
- [12] Hou Y, Wang Q, Han B, et al. CD36 promotes NLRP3 inflammasome activation via the mtROS pathway in renal tubular epithelial cells of diabetic kidneys. *Cell Death Dis.* 2021;12(6):523. doi: [10.1038/s41419-021-03813-6](https://doi.org/10.1038/s41419-021-03813-6).
- [13] Rong Q, Han B, Li Y, et al. Berberine reduces lipid accumulation by promoting fatty acid oxidation in renal tubular epithelial cells of the diabetic kidney. *Front Pharmacol.* 2021;12:729384. doi: [10.3389/fphar.2021.729384](https://doi.org/10.3389/fphar.2021.729384).
- [14] Yokoi H, Yanagita M. Targeting the fatty acid transport protein CD36, a class B scavenger receptor, in the treatment of renal disease. *Kidney Int.* 2016;89(4):740–742. doi: [10.1016/j.kint.2016.01.009](https://doi.org/10.1016/j.kint.2016.01.009).
- [15] Yang X, Okamura DM, Lu X, et al. CD36 in chronic kidney disease: novel insights and therapeutic opportunities. *Nat Rev Nephrol.* 2017;13(12):769–781. doi: [10.1038/nrneph.2017.126](https://doi.org/10.1038/nrneph.2017.126).
- [16] Kennedy DJ, Chen Y, Huang W, et al. CD36 and Na/K-ATPase- α 1 form a proinflammatory signaling loop in kidney. *Hypertension.* 2013;61(1):216–224. doi: [10.1161/HYPERTENSIONAHA.112.198770](https://doi.org/10.1161/HYPERTENSIONAHA.112.198770).
- [17] Samovski D, Sun J, Pietka T, et al. Regulation of AMPK activation by CD36 links fatty acid uptake to β -oxidation. *Diabetes.* 2015;64(2):353–359. doi: [10.2337/db14-0582](https://doi.org/10.2337/db14-0582).
- [18] Yoshida Y, Jain SS, McFarlan JT, et al. Exercise- and training-induced upregulation of skeletal muscle fatty acid oxidation are not solely dependent on mitochondrial machinery and biogenesis. *J Physiol.* 2013;591(18):4415–4426. doi: [10.1113/jphysiol.2012.238451](https://doi.org/10.1113/jphysiol.2012.238451).
- [19] Zeng S, Wu F, Chen M, et al. Inhibition of fatty acid translocase (FAT/CD36) palmitoylation enhances hepatic fatty acid β -oxidation by increasing its localization to mitochondria and interaction with long-chain Acyl-CoA synthetase 1. *Antioxid Redox Signal.* 2022;36(16–18):1081–1100. doi: [10.1089/ars.2021.0157](https://doi.org/10.1089/ars.2021.0157).
- [20] Shen S, Ji C, Wei K. Cellular senescence and regulated cell death of tubular epithelial cells in diabetic kidney disease. *Front Endocrinol.* 2022;13:924299. doi: [10.3389/fendo.2022.924299](https://doi.org/10.3389/fendo.2022.924299).
- [21] Mima A. Mitochondria-targeted drugs for diabetic kidney disease. *Heliyon.* 2022;8(2):e08878. doi: [10.1016/j.heliyon.2022.e08878](https://doi.org/10.1016/j.heliyon.2022.e08878).
- [22] Susztak K, Ciccone E, McCue P, et al. Multiple metabolic hits converge on CD36 as novel mediator of tubular epithelial apoptosis in diabetic nephropathy. *PLoS Med.* 2005;2(2):e45. doi: [10.1371/journal.pmed.0020045](https://doi.org/10.1371/journal.pmed.0020045).
- [23] Son NH, Basu D, Samovski D, et al. Endothelial cell CD36 optimizes tissue fatty acid uptake. *J Clin Invest.* 2018;128(10):4329–4342. doi: [10.1172/JCI99315](https://doi.org/10.1172/JCI99315).
- [24] Jeong JY, Jeoung NH, Park KG, et al. Transcriptional regulation of pyruvate dehydrogenase kinase. *Diabetes Metab J.* 2012;36(5):328–335. doi: [10.4093/dmj.2012.36.5.328](https://doi.org/10.4093/dmj.2012.36.5.328).
- [25] Nahlé Z, Hsieh M, Pietka T, et al. CD36-dependent regulation of muscle FoxO1 and PDK4 in the PPAR Delta/beta-mediated adaptation to metabolic stress. *J Biol Chem.* 2008;283(21):14317–14326. doi: [10.1074/jbc.M706478200](https://doi.org/10.1074/jbc.M706478200).
- [26] Song X, Liu J, Kuang F, et al. PDK4 dictates metabolic resistance to ferroptosis by suppressing pyruvate oxidation and fatty acid synthesis. *Cell Rep.* 2021;34(8):108767. doi: [10.1016/j.celrep.2021.108767](https://doi.org/10.1016/j.celrep.2021.108767).
- [27] Park BY, Jeon JH, Go Y, et al. PDK4 deficiency suppresses hepatic glucagon signaling by decreasing cAMP levels. *Diabetes.* 2018;67(10):2054–2068. doi: [10.2337/db17-1529](https://doi.org/10.2337/db17-1529).